

## Decarburisation Effect on Hardened Strip Steel Fastening Components

Karli JAASON<sup>1\*</sup>, Priidu PEETSALU<sup>1</sup>, Mart SAARNA<sup>1</sup>, Priit KULU<sup>1</sup>, Jüri BEILMANN<sup>2</sup>

<sup>1</sup>Tallinn University of Technology Department of Materials Engineering, Ehitajate tee 5, 19086 Tallinn Estonia

<sup>2</sup>AS Norma, Laki 14, 10621 Tallinn, Estonia

crossref <http://dx.doi.org/10.5755/j01.ms.22.1.7467>

Received 29 June 2014; accepted 20 February 2015

Heat treatment is widely used for high reliability fastening components such as buckles and brackets. The current study focuses on mass production of safety components which are fineblanked from sheet metal, austempered and chromium electroplated. Electroplating together with stamping defects may lead to unexpected brittle failure of the component. It is widely known that during austenitisation, decarburisation could avoid brittle failure and, therefore, slight decarburisation is recommended. There is little information how much mass production is influenced by decarburisation and where the limits are. The current study has two goals. The first one focuses on the extent of decarburisation effect on the part properties, and the second aims to find the optimum furnace setting for the product type used in the study. Also, it is necessary to choose a reliable decarburisation control method for austempered components. The effect on material grades was analyzed by using three steel alloys with carbon content of 0.37 wt.%, 0.47 wt.% and 0.62 wt.%. The specimens were austempered to hardness 45–51 HRC under endothermic protective atmosphere. To gain different decarburisation levels, two gas set-ups were used. Infrared gas analyzer was used to measure CO and CO<sub>2</sub> content in the furnace gas. Three characteristics of the specimens were evaluated: hardness, rupture strength and brittleness. The depth of the decarburisation was determined by three different approaches according to standard EN ISO 3887. Based on the results, the spectrographic method is the most reliable for determining the depth of decarburisation. This study reveals that higher surface decarburisation has a positive effect on the ductility and no effect on the rupture strength of the component. The material with carbon content of 0.62 wt.% is the most sensitive to decarburisation. During mass production, the inaccuracy of hardness measuring raises which results in the inaccuracy of salt bath temperature regulation. For the used thermal cycle, the furnace gas carbon potential 0.30–0.40 has to be used to ensure expected performance of fastening products.

*Keywords:* austempering, endothermic atmosphere, decarburisation, chromium plating, hydrogen embrittlement.

### 1. INTRODUCTION

This study focuses on a safety fastening products that in a crash situation have to resist to dynamic load and have to withstand plastic deformation before failure. These fastening components are manufactured from strip steel by fineblanking and die forming. During this process, micro cracks are formed on the cut surface. Stamped surface is the surface where stresses are concentrated and deformation starts. To assure required mechanical properties of the steel components austempering is used. Austempering process is the isothermal transformation of a ferrous alloy at a temperature below that of pearlite formation and above that of martensite formation. The final structure obtained by the austempering process is bainite [1]. Hardness between 45–51 HRC (Yield strength 1200–1600 MPa) is required after the heat treatment. Finally, Ni-Cr electroplating assures components' appearance and corrosion resistance. During electroplating, hydrogen is introduced into the part which may result in hydrogen embrittlement. Previous experience in component mass production has shown that besides other properties, decarburisation is an important characteristic to be considered. Decarburisation of steel is defined as carbon loss from steel surface during heat treatment in gaseous atmospheres [1, 2]. The reactions between gas and steel

surface in the furnace are temperature dependent because of the diffusion process [3, 4]. The intensity and balance of the reactions depend on time and temperature, therefore, the depth of decarburisation is a result from the used thermal cycle [4, 5, 6].

Many expert analyses have shown product failures resulted from brittle surface, although other properties met the requirements. It is known that decarburisation affects hardened steel properties by increasing the material's resistance to brittle fracture [7]. Previous studies do not specify what extent of decarburisation should be used on the parts. The present study focuses on the effect of surface decarburisation on the functional properties of electroplated products. There is a demand for knowledge how to choose optimum decarburisation to assure tensile strength and ductility properties of components. Standard EN ISO 3887 gives three different methods for determining the depth of decarburisation. However, a reliable method has to be chosen considering the specific case.

### 2. EXPERIMENTAL

#### 2.1. Specimens and materials

The design of the specimens was originated from the existing fastening products. One end of the specimen was designed to be fixed with a pin. The opposite end was designed to be clamped with tensile testing machine

\* Corresponding author. Tel.: +372-5907-9440; fax: +372-6500-297.  
E-mail address: karli.jaason@gmail.com (K. Jaason)

gripper. The specimens were made from 21 mm x 50 mm steel band with 3 mm in thickness. The design of the specimens is shown on Fig. 1. The material grades were selected based on steel carbon content and the ability to be austempered in the range of 45–51 HRC. The material chemical compositions are given in Table 1.

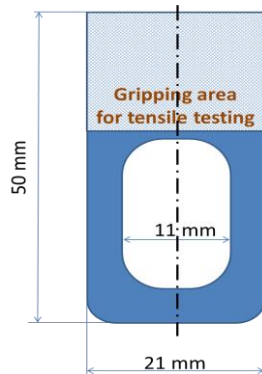


Fig. 1. Design of specimens used in testing

The specimens were fineblanked from steel band and austempered. Then the surface was treated by smooth grinding and then electroplated with bright Ni–Cr. The thickness of the Ni–Cr electroplating layer on specimens was 12  $\mu\text{m}$ –20  $\mu\text{m}$ . Electroplating process introduces hydrogen into hardened material causing embrittlement [8, 9]. For this reason, hydrogen embrittlement removal procedure was executed on specimens in air atmosphere for 4 hours at 210  $^{\circ}\text{C}$ .

Table 1. Chemical composition of steels used (wt.%)

Sample	C	Mn	S	Al	Cr	B
Mat I	0.62	0.63	0.002	0.020	0.23	-
Mat II	0.47	0.69	0.001	0.005	0.26	-
Mat III	0.37	1.28	0.004	0.036	0.71	0.0012

## 2.2. Industrial austempering equipment

The study was carried out in a continuous belt-type industrial austempering furnace. The furnace line consists of the loading area, austenitising furnace, salt quench tank and water treatment tank. The austenitising furnace is a muffle type furnace with installed electrical heating power of 180 kW. The furnace is divided into four heating zones, the temperatures of which are controlled through thermocouple system. The total length of the furnace heating zone is 3.74 meters and the muffle cross-section is about 740 mm x 270 mm. The respective heating curve of the parts in the furnace was measured separately with a long K-type thermocouple. The thermocouple was fed through the furnace between parts and the temperature drive was recorded.

The furnace uses endothermic protective gas atmosphere from a standalone gas generator. The hot endogas from the gas generator is cooled down to 50  $^{\circ}\text{C}$ –80  $^{\circ}\text{C}$  and fed through a piping system into the furnace. The furnace gas inlet is from the rear and the furnace has no atmosphere circulation fan. The furnace gas system is monitored with Siemens infrared ULTRAMAT 32 gas analyser which measures the content of CO and CO<sub>2</sub>. The furnace zones and salt bath set-up temperatures are given in Table 2.

Table 2. Furnace zone set-temperatures and used salt temperature

	Zone I, $^{\circ}\text{C}$	Zone II, $^{\circ}\text{C}$	Zone III, $^{\circ}\text{C}$	Zone IV, $^{\circ}\text{C}$	Salt, $^{\circ}\text{C}$
Set 1	840	880	885	890	313
Set 2	840	880	885	890	312

The test was carried out with two different gas set-ups with the purpose to achieve minimum and maximum decarburisation during the furnace thermal cycle. The thermal cycle of specimens in the furnace was kept constant. The endogas quantity was kept in the range of 18 m<sup>3</sup>/h and 19 m<sup>3</sup>/h. To vary the decarburisation intensity of endogas, the air/gas ratio fed into the gas generator was adjusted. The endogas generator parameters are given in Table 3. Hereby in Set 2, 0.24 m<sup>3</sup>/h methane was additionally fed into the furnace to reduce decarburisation intensity. Before the test run, the furnace atmosphere was left to stabilise for two hours. During the test, the gas analyser readings for CO and CO<sub>2</sub> were recorded. The gas analyser results are given in Table 3.

Table 3. Gas generator set-up and furnace gas analysis results

	Air, m <sup>3</sup> /h	CH <sub>4</sub> , m <sup>3</sup> /h	Ratio, CH <sub>4</sub> /air	CO, %	CO <sub>2</sub> , %
Set 1	12.0	3.6	3.3	17.60	1.850
Set 2	10.5	4.0	2.6	20.18	0.285

## 2.3. Specimens testing

After austempering, the hardness of specimens was measured and the depth of decarburisation was determined by the spectrographic, microhardness and microstructural methods. Rupture strength and bending test were performed after Ni–Cr electroplating. The minimum requirement for rupture strength is 22.0 kN and for bending test 30 $^{\circ}$ . The bending requirement is experiential as the parts which do not resist 30 $^{\circ}$  bending, start to vary in rupture strength.

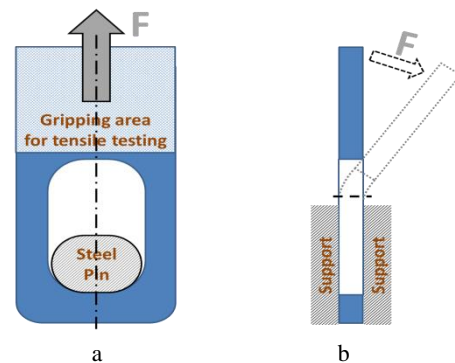


Fig. 2. Rupture test (a) and bending test (b) scheme

The hardness of the specimens was measured with Indentec 4150LK Rockwell hardness testing device in C-scale. The rupture strength test was executed on a quasistatic tensile testing machine Housefield H100K with the testing speed of 100 mm/min. The bending test was performed by fixing one end of the specimen in the rigid clamp. The force was applied with lever to the other end in order to bend the specimen around cylindrical mandrel with the radius of 3 mm. The angle of specimen fracture was fixed from the bending radius scale. The rupture test and bending test schemes are given on Fig. 2.

## 2.4. Determination of decarburisation depth

The depth of decarburisation was determined according to standard EN ISO 3887, which gives three different methods: micrograph, microhardness and chemical composition [10]. The micrograph and microhardness methods require microsection of the surface area of the specimen. The chemical composition method requires a steel carbon content measuring instrument.

For microsections, the specimens were cut and hot mounted in plastic then grinded and polished. Final polishing was done by using 0.05  $\mu\text{m}$  Buehler Masterpolish suspension. To reveal the microstructure, the nital etchant (nitric acid, 3 wt.%) was used [11]. The microstructure was examined using optical microscope Axiovert 25. The micrograph method was used for evaluating the difference in etched microstructure near the surface of the specimens. Based on the existence of ferrite or the distribution of carbides in microstructure, the decarburised layer was evaluated. The microhardness method was used to measure the Vickers hardness gradient across the surface layer. The depth of decarburisation of the surface was determined by measuring the distance up to the point where core hardness was reached. The microhardness was tested on microsection with the HV0.1.

For the chemical composition method, the carbon changing gradient was obtained. The surface layers of the specimen were removed step-by-step and the carbon content of the layers was measured. The Spectrolab optical emission spectrometry (OES) measurement instrument was used for determining carbon content. The thickness of the removed surface layer was measured with a micrometer and a corresponding graphical output was composed. The measurements were taken from the gripping area of the specimen (Fig. 2).

## 3. RESULTS AND DISCUSSION

To characterize the decarburisation of specimens in the furnace, the corresponding heating curve was measured. The heating curve is given on Fig. 3, where the steel phase transformation temperature line  $A_{c1}$  (727  $^{\circ}\text{C}$ ) is marked with an orange dotted line. Line  $A_{c1}$  is the start of carbon diffusion in austenite, which indicates the start of the intensive diffusion and decarburisation process [4, 5]. The results show that the specimens were 23 minutes above  $A_{c1}$  temperature wherein 8 minutes at the soaking temperature of  $890 \pm 10$   $^{\circ}\text{C}$ . The heating curve is necessary for linking the furnace heating cycle and the depth of decarburisation of steel. The heating curve allows predicting the depth of decarburisation of the parts without direct testing.

Three different methods from standard EN ISO 3887 were used to determine the depth of decarburisation of the specimens. It occurred that the methods are not one-to-one compatible as the used determination techniques are different.

The results of the chemical composition method are presented on Fig. 4. It is evident that in the first gas setup (Set 1) decarburisation was more intensive than in the second (Set 2). The decarburisation of the surface was detected on all three alloys, except gas setup 2 (Set 2) of

material I (Mat III). In case of Mat III and gas Set 2, slight carburisation (carbon addition) on the specimens was detected. The results demonstrate the difference in decarburisation related to alloy carbon content.

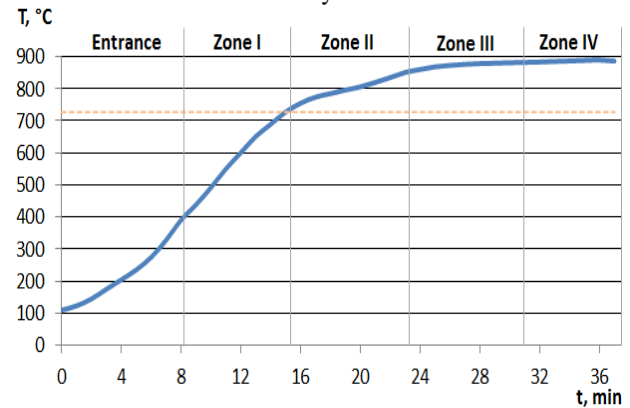


Fig. 3. The referring heating curve of specimens

The microhardness and micrograph methods confirm decarburisation of surface which was detected with the spectral method. When comparing different methods, the chemical composition (Fig. 4) and microhardness (Fig. 5) method have similar graphical outputs. The micrographs on Fig. 6 show differences in microstructures of the surface layers.

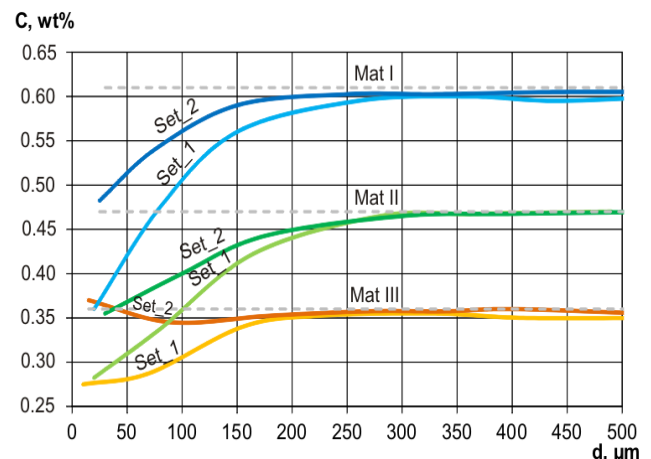


Fig. 4. Decarburisation of specimens measured with spectrographic method ( $d$  – distance from surface)

In Table 4, the determined range of total decarburisation depth ( $d_4$ ) for all three methods is given. When comparing the results from Mat I and Set 1, the results are 275  $\mu\text{m}$ , 200  $\mu\text{m}$  and 150  $\mu\text{m}$ . It shows the difference between the methods. Hereby, in case of Set 2, it was not possible to determine the depth of decarburisation with the micrograph method (Fig. 6). The micrograph method depends a lot on the specimen's preparation and etching result. This method is acceptable only to a certain extent of decarburisation.

When the carbon content difference between the surface and core is inconsiderable, the method is not applicable. The spectral method gives a good quantitative result about decarburisation as it measures the direct carbon content value. The microhardness method remains in between as it is quantitative, but the resolution depends on the variance of carbon content. Hardness, rupture strength and bending tests were performed. The average results of 10 samples are given in Table 5 and Table 6.

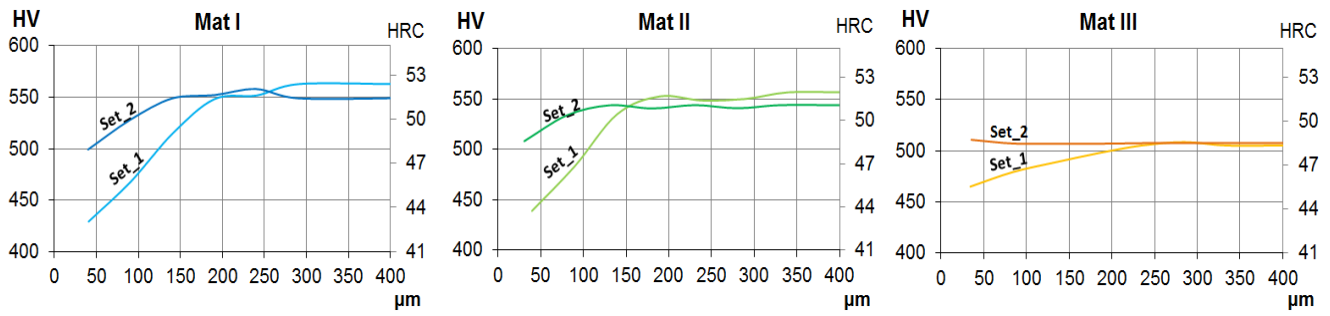


Fig. 5. Decarburisation depths for Mat I, Mat II and Mat III with microhardness method (HV0.1)

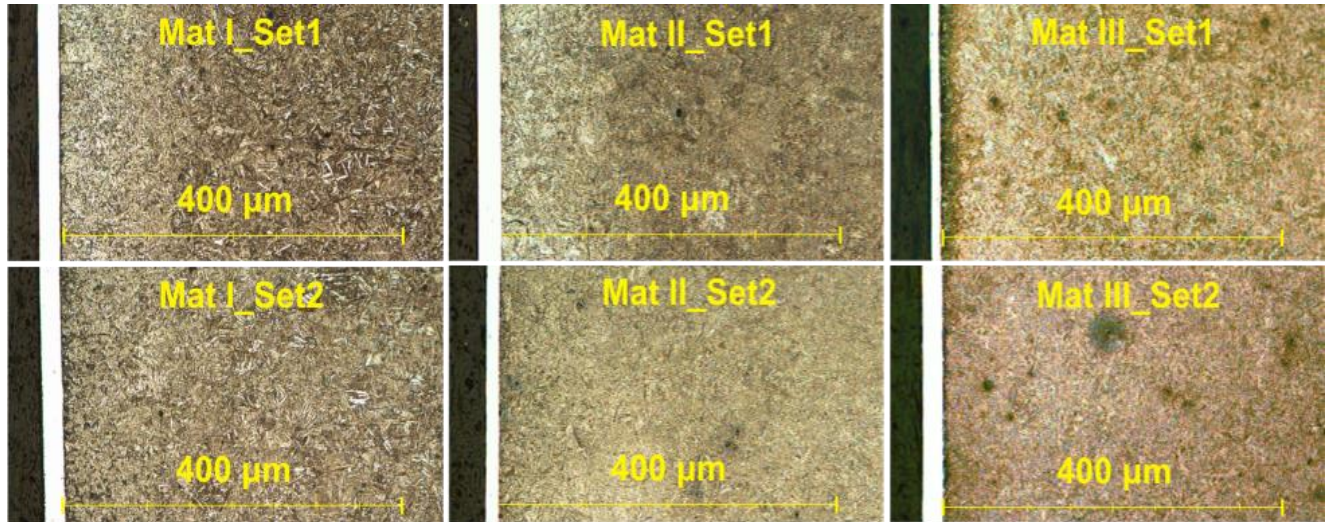


Fig. 6. Micrograph of the specimens for micrograph method

Table 4. Depth of total decarburisation ( $d_4$ )

Sample	Chemical $d_4$ , $\mu\text{m}$		Microhardness $d_4$ , $\mu\text{m}$		Micrograph $d_4$ , $\mu\text{m}$	
	Set_1	Set_2	Set_1	Set_2	Set_1	Set_2
Mat I	275	200	200	150	150	-
Mat II	275	275	175	125	125	-
Mat III	175	100	200	50	100	-

The hardness of specimens was measured from the surface and core

The results in Table 5 show a difference in hardness between the surface and core. The hardness difference is in accordance with the decarburisation of the surface. According to the results in Table 5, the Rockwell hardness difference between the surface and core can be up to 3 HRC units. This effect has to be considered carefully in adjustment of austempering process parameters. The hardness of parts is controlled by adjusting the quenching bath salt temperature. When increasing hardness, steel becomes more susceptible to brittleness. Hereby, it is highly recommended to consider the effect that the decarburized layer has on hardness measuring.

Table 5. Hardness results

Sample	HRC surface		HRC core	
	Set_1	Set_2	Set_1	Set_2
Mat I	$48.5 \pm 1.2$	$50.0 \pm 1.2$	$51.0 \pm 1.2$	$51.0 \pm 1.2$
Mat II	$47.5 \pm 1.2$	$50.0 \pm 1.2$	$51.0 \pm 1.2$	$51.0 \pm 1.2$
Mat III	$45.0 \pm 1.2$	$47.0 \pm 1.2$	$48.0 \pm 1.2$	$48.0 \pm 1.2$

The bending test shows material's resistance to plastic deformations. The test results are given in Table 6. There is a clear difference between the results of Set 1 and Set 2. The specimens with greater depth of decarburisation (Set 2) demonstrate better resistance to plastic deformation. It is evident that the lower the alloy carbon content is, the better the material's resistance to deformation is. Therefore, the higher the carbon content in the alloy is, the more significance the effect of decarburisation has.

Table 6. Bending test and rupture force

Sample	Bending test, $^\circ$		Rupture F, kN	
	Set_1	Set_2	Set_1	Set_2
Mat_I	$47 \pm 3$	$36 \pm 3$	$28.2 \pm 0.2$	$28.9 \pm 0.2$
Mat_II	$59 \pm 3$	$47 \pm 3$	$28.5 \pm 0.2$	$29.0 \pm 0.2$
Mat_III	$59 \pm 3$	$49 \pm 3$	$26.5 \pm 0.2$	$26.8 \pm 0.2$

The results of the rupture test are seen in Table 6. Decarburisation has no considerable effect on rupture strength. The main factor here is the carbon content of the alloy. Mat III has lower results than Mat II and Mat I. Table 5 shows that the hardness of Mat III was proportionally lower, which explains the rupture strength difference.

Brittleness is an important characteristic of fastening parts as they have to resist dynamic forces or impact. The bending test in this study is the primary method to evaluate the brittleness of the specimens after Ni-Cr plating. The results in Table 6 and Set 1 show better resistance to

bending. The Mat I, in Set 2 with the total depth of decarburisation of 200 µm meets the bending test minimum requirement. Based on Fig. 4, the furnace gas carbon potential during test Set 2 was less than 0.40. In Set 1 the carbon potential is less than 0.30 and causes hardness difference up to 3 HRC units between surface and core. The furnace carbon potential of 0.40–0.30 is the optimal allowed decarburisation atmosphere to use on fastening products.

#### 4. CONCLUSION

The current study shows that the decarburisation of surface in the austempering process is a critical characteristic for Ni-Cr electroplated fastening products' ductility. The decarburisation of steel surface increases product's resistance to plastic deformations in crash situations. The rupture strength of the components was not affected by the decarburisation limits tested in the current paper.

Decarburisation is beneficial to the part's ductility. Hereby it can increase brittleness if the salt quench bath temperature regulation is based on inaccurate measurement of hardness from the surface of the material. In the study, 3 HRC unit higher hardness value was obtained from the core than from the surface. Higher core hardness is critical as it increases the brittleness risk of hardened steel.

Three different methods from EN ISO 3887 were studied for determining the depth of decarburisation. The comparison of them shows that the chemical composition method is the most reliable for evaluating decarburisation of austempered steel.

For the specific thermal cycle, the furnace gas Set 2 with carbon potential of 0.30–0.40 has to be used to ensure expected performance of fastening products.

#### Acknowledgments

This research was supported by European Social Fund of Doctoral Studies and Internationalization Programme

DoRa. The author would like to express his gratitude to company Norma AS for its support and cooperation.

#### REFERENCES

1. **Totten, G.E.** Steel Heat Treatment Handbook, Chapter 2: Classification and Mechanisms of Steel Transformation, 2006.
2. **Totten, G. E.** Steel Heat Treatment Handbook Chapter 7: Heat Treatment with Gaseous Atmospheres, 2006.
3. ASM International Handbook, Heat Treating, Vol 04, 1991.
4. **Dejun, Li., Anghelina, D., Burzic, D., Zamberger, J., Kienreich, R., Schifferl, H., Krieger, W., Kozeschnik, E.** Investigation of Decarburisation in Spring Steel Production Process *Steel Research International* 80 (4) 2009: pp. 298–304.
5. **Dejun, Li., Anghelina, D., Burzic, D., Krieger, W., Kozeschnik, E.** Investigation of Decarburisation in Spring Steel Production Process – Part II: Simulation *Steel Research International* 80 (4) 2009: pp. 304–310.
6. **Sangwoo, C., Sybrand van der, Z.** Prediction of Decarburized Ferrite Depth of Hypoeutectoid Steel with Simultaneous Oxidation *ISIJ International* 52 (4) 2012: pp. 549–558.
7. **Illina, V.P.** Effect of Surface Decarburisation on the Susceptibility of High-strength Steel 38Kh5MSFA to Brittle Fracture *Material Science and Heat Treatment* 41 1999: pp. 20–21.
8. **Peetsalu, P., Mikli, V., Ratas, K., Kulper, E., Jaason, K.** Bainitic Structure Effect on Hydrogen Embrittlement *Journal of The Japan Society for Heat Treatment* 49 2009: pp. 592–595.
9. **Oriani, R.A., Hirth, J.P., Smialowski, M.** Hydrogen Degradation of Ferrous Alloys. William Andrew Publishing/Noyes, New Jersey, 1985.
10. EN ISO 3887 Steels – Determination of Depth of Decarburisation, 2003.
11. ASM International Handbook, Metallography and Microstructures, vol. 09. ASM International, 1991.